Technical note: Displacement variance of a solute particle in heterogeneous confined aquifers with random aquifer thickness fields

Ching-Min Chang[1], Chuen-Fa Ni[1], Chi-Ping Lin[2], and I-Hsien Lee[2]

[1]Graduate Institute of Applied Geology, National Central University, Taoyuan, Taiwan

[2]Center for Environmental Studies, National Central University, Taoyuan, Taiwan

Correspondence: Chuen-Fa Ni (nichuenfa@geo.ncu.edu.tw)

Abstract.

In this work, the variability of regional-scale transport of inert solutes in heterogeneous confined aquifers of variable thickness is quantified by the variance of the displacement of a solute particle. Variability in solute displacement is attributed to variability in hydraulic conductivity and aquifer thickness. A general stochastic methodology for deriving the variance of the displacement of a solute particle based on the convection velocity of solute particles, developed from the relationship between the two-dimensional depth-averaged solute mass conservation equation and the Fokker-Planck equation, is given. Explicit results for the solute displacement variance in the mean flow direction for the case of advection-dominated solute transport are obtained assuming that the fluctuations in log hydraulic conductivity and log thickness of the confined aquifer are second-order stationary processes. The results show that variation in hydraulic conductivity and aquifer thickness can lead to nonstationarity in the covariance of flow velocity, making longitudinal macrodispersion anomalous and increasing linearly with travel time at large distances.

1 Introduction

It is widely accepted that the variability of solute movement in heterogeneous aquifers is controlled primarily by the spatial variability of groundwater flow fields (e.g., Dagan, 1989; Gelhar, 1993; Rubin, 2003). Much work on the stochastic analysis of solute transport in heterogeneous porous formations has focused on relating the spatial variability of the hydraulic conductivity field to that of the flow velocity field, and thus to the spatial variability of the displacement of a solute particle. However, natural aquifers at regional scales often exhibit nonuniform aquifer thickness (e.g., Masterson et al., 2013; Zamrsky et al., 2018; DeSimone et al., 2020), and spatial variability in the aquifer thickness field has also been shown to have an important influence on flow field variability (e.g., Hantush, 1962; Cuello and Guarracino, 2020; Chang et al., 2021). Thus, the underlying motivation for this work is to provide an analytical stochastic method for improved quantification of the variability of solute displacement at the regional scale in heterogeneous aquifers under more realistic field conditions, i.e., taking into account the effects not only of the spatial variation of the hydraulic conductivity field but also of the thickness field of the confined aquifer.

At a regional scale, the lateral extent of the confined aquifer is much greater than the thickness of the formation. Therefore, it is more practical to view the flow and solute transport processes in confined aquifers at the regional scale as essentially two-dimensional, areal processes. In the traditional approach to the essentially horizontal flow, the stochastic description of flow and solute transport processes is related to the stochastic properties of transmissivity (e.g., Dagan, 1982; 1984), where the transmissivity is the line integration of hydraulic conductivity over the depth of the formation at a given point. However, in reality, transmissivity measurements from field tests give a value of integrated hydraulic conductivity over a larger volume than the range used for the line integration of hydraulic conductivity at a single point. This means that the field tests performed for the transmissivity measurements include more of the heterogeneity in the formation than that encountered over the depth of the formation at a single point. This would result in a reduction in the variance of transmissivity and an overestimation of the integral scale of transmissivity compared to values predicted from the line integration of hydraulic conductivity. Consequently, using the stochastic properties of transmissivity may not provide an accurate interpretation of solute movement at a regional scale.

Rather than using the stochastic properties of transmissivity, this work uses the stochastic properties of hydraulic conductivity and thickness of the confined aquifer to interpret the variability of solute movement at a regional scale using a hydraulic approach (or essentially horizontal flow approach) (Bear, 1979; Bear and Cheng, 2010). That is, in this approach, the variability in solute movement is due to variations in hydraulic conductivity and aquifer thickness.

The traditional approach to regional groundwater flow problems introduces the transmissivity parameter to describe the ability of a confined aquifer to transmit water throughout its saturated thickness. The effect of the thickness of the aquifer is implicitly reflected in the transmissivity parameter. It is very difficult to assess the effect of thickness on the flow field and thus on solute transport at a regional scale. The stochastic approach presented here provides an efficient and rational way to analyze flow and solute transport fields affected by the non-uniform thickness of confined aquifers, which has not been previously presented in the literature. This work shows that variability in aquifer thickness can lead to nonstationarity in hydraulic head fields and thus to nonstationary flow velocity fields and anomalous longitudinal dispersion. This implies that neglecting the variability of aquifer thickness when predicting the longitudinal displacement of solutes at large times can lead to a significant underestimation of longitudinal dispersion. The stochastic theory presented here improves quantification of the variance of the solute displacement in natural confined aquifers of random thickness fields.

In the present work, the convection velocity of solute particles is first developed based on the relationship between the two-dimensional depth-averaged solute mass conservation equation and the Fokker-Planck equation, so that the convection velocity can explicitly reflect the effects of hydraulic conductivity and aquifer thickness. Using the perturbation approach to solute convection velocity, the covariance function of solute convection velocity is then developed, which allows a general expression for the variance of the displacement of a solute particle in the mean flow direction to be developed. A closed-form expression for the solute displacement variance is also developed for the case where solute transport is dominated by advection and the random fields of log conductivity and log thickness of the confined aquifer are second-order stationary. Finally, the influence of variations in log hydraulic conductivity and log aquifer thickness on the variability of solution displacement is analyzed.

2 Mathematical formulation of the problem

Consider here the steady flow of a fluid carrying an inert solute through a heterogeneous confined aquifer with variable thickness. When constituents are well mixed throughout the thickness of the aquifer (depth of flow) and fluid flow through an aquifer occurs on a regional scale, with the lateral extent of the formation much greater than the thickness of the formation, it is appropriate to view the flow and solute transport processes as essentially two-dimensional. In this work, the two-dimensional solute transport process in heterogeneous confined aquifers is quantified by using moments of solute particle displacement in the Lagrangian framework (e.g., Dagan, 1982; 1984), where the particle displacement can be defined as

$$\frac{d\boldsymbol{X}}{dt} = \boldsymbol{V}_c \tag{1}$$

In Eq. (1), $\boldsymbol{X}$ (= (X_1, X_2)) is the displacement and $\boldsymbol{V}_c$ (= (V_{c_1}, V_{c_2})) is the convection velocity of the solute particle.

The displacement of the solute particles in Eq. (1) consists of two components: one originates from convection through the fluid and the other is associated with the transport process at the pore scale. This means that the statistical moments of particle displacement cannot be determined directly from the statistical moments of flow velocity. The convection velocity of the solute particle in Eq. (1) can be obtained from the relationship between the two-dimensional depth-averaged equation for the conservation of solute mass and the Fokker-Planck equation as follows:

$$\frac{dX_i}{dt} = \frac{1}{n}\tilde{q}_i(\boldsymbol{X}) + \left[\frac{1}{n}\tilde{D}_i(\boldsymbol{X})\frac{\partial}{\partial x_i}\ln B(\boldsymbol{X}) + \frac{1}{n}\frac{\partial}{\partial x_i}\tilde{D}_i(\boldsymbol{X})\right] + \sqrt{\frac{2}{n}\tilde{D}_i(\boldsymbol{X})}\,\frac{dW}{dt} \qquad i = 1,2. \tag{2}$$

where n is the porosity, $\tilde{D}_i$, and $\tilde{q}_i$ represent the depth-averaged dispersion coefficient and depth-averaged specific discharge in the x_i direction, respectively, B is the thickness of a confined aquifer, and W denotes a Wiener process. The details of the development of Eq. (2) are given in Appendix A.

From the right-hand side of Eq. (2), it can be seen that the first term represents the convection velocity of the flow, the second and third terms are associated with pore-scale dispersion, which includes the effects of local heterogeneity of aquifer thickness and dispersion coefficient, respectively, and the last term is associated with a Brownian motion type diffusion process. Equation (2) provides a basic basis for evaluating the statistical moments of solute particle displacement.

In this study, the fields (or processes) of hydraulic conductivity $K(x_1,x_2)$ and thickness of the confined aquifer $B(x_1,x_2)$ are considered spatially random, and therefore a random flow field and a random particle displacement field. It is also assumed that the mean fluid flow is uniform and unidirectional in the x_1-direction (i.e., $<\boldsymbol{X}> = (<X_1>, 0)$) and that the spatial variation of the depth-averaged dispersion coefficients and the Brownian motion type diffusion process are negligible. This simplifies Eq. (2) to

$$\frac{dX_i}{dt}=\frac{1}{n}\tilde{q}_i(\boldsymbol{X})+\frac{1}{n}\tilde{D}_i\frac{\partial}{\partial x_i}\ln B(\boldsymbol{X}) \qquad i=1,2. \tag{3}$$

Note that the assumption of uniform mean flow in the x_1-direction implies that the gradient of the mean depth-averaged hydraulic head is constant in the x_1-direction and zero in the x_2-direction (Chang et al. 2021).

By analogy with Butera and Tanda (1999), extending Eq. (3) in Taylor series around $<\boldsymbol{X}>$ in the x_1-direction yields

$$\frac{dX_1}{dt}=\frac{1}{n}\tilde{D}_1\left[\frac{\partial \Phi(<X_1>,0)}{dx_1}+\frac{d^2\Phi(<X_1>,0)}{dx_1^2}X_1^{'}+\frac{d\beta(<X_1>,0)}{dx_1}\right]+<\tilde{v}_1>+v_1(<X_1>,0), \tag{4}$$

where $X_1' = X_1 - \langle X_1 \rangle$, $\Phi = \langle \ln B \rangle$, $\beta = \ln B - \langle \ln B \rangle$, $v_1 = \tilde{v}_1 - \langle \tilde{v}_1 \rangle$, $\langle \tilde{v}_1 \rangle$ = constant, and $\tilde{v}_1 = \tilde{q}_1 / n$. Note that due to the assumption of uniform mean flow in the x_1-direction, the term $\frac{d \langle \tilde{v}_1 \rangle}{dx_1} X_1'$ has been removed from Eq. (4). Equation (4) reveals that

$$\frac{d \langle X_1 \rangle}{dt} = \frac{1}{n} \tilde{D}_1 \frac{d\Phi(\langle X_1 \rangle, 0)}{dx_1} + \langle \tilde{v}_1 \rangle, \tag{5a}$$

$$\frac{dX_1'}{dt} - \frac{\tilde{D}_1}{n} \frac{d^2\Phi(\langle X_1 \rangle, 0)}{dx_1^2} X_1' = \frac{\tilde{D}_1}{n} \frac{d\beta(\langle X_1 \rangle, 0)}{dx_1} + v_1(\langle X_1 \rangle, 0). \tag{5b}$$

Equations (5a) and (5b) describe the mean and fluctuation, respectively, of the displacement of the solute particles. By the solution of Eq. (5), the variance of the solute displacement in the x_1-direction (the mean flow direction) can be evaluated in the frame, (e.g., Dagan, 1984; 1989)

$$X_{11}(t) = \langle X_1'(t) X_1'(t) \rangle. \tag{6}$$

It is important to recognize the validity of the assumption of a first order perturbation of X_1. The first-order approximation for representing the depth-averaged hydraulic head perturbation, and hence the solute displacement perturbation, should be applied to porous formations where the standard deviation of the random fluctuations of the log hydraulic conductivity is less than 1. However, Zhang and Winter (1999) report in a Monte Carlo simulation study that it is accurate for the solutions of the head moment for the value of the variance of the log conductivity of up to 4.38. A similar finding from comparing moments of hydraulic head with results of numerical Monte Carlo simulations is also reported in Guadagnini and Neuman (1999) for highly heterogeneous media with a variance of log conductivity from 2 to 4.

In the case where the thickness of the aquifer is a slowly spatially varying process (e.g., a second-order stationary process), the terms $d\Phi/dx_1$ and $d^2\Phi/dx_1^{\,2}$ in Eq. (5) may be neglected, and, consequently, Eq. (5) reduces to

$$\frac{d < X_1 >}{dt} = <\tilde{v}_1>, \tag{7a}$$

$$\frac{dX_1^{'}}{dt} = \frac{\tilde{D}_1}{n}\frac{d\beta(<X_1>,0)}{dx_1} + v_1(<X_1>,0). \tag{7b}$$

Equation (7b) implies that the variability of the particle displacement is determined by the gradient of the variation of the aquifer thickness fields and the variability of the flow velocity. Note that when flowing through a confined aquifer with variable thickness, the variability in flow velocity is influenced by both the variation in log conductivity and log thickness fields (Chang et al., 2021). This means that the variability of v_1 in Eq. (7b) depends on both the variation of log conductivity and log aquifer thickness.

Using the solution of Eq. (7),

$$X_1^{'}(t) = \int_0^t \Big[\frac{\tilde{D}_1}{n}\frac{d\beta}{dx_1}(<\tilde{v}_1> s,0) + v_1(<\tilde{v}_1> s,0)\Big] ds, \tag{8}$$

the variance of the solute displacement in the mean flow direction in Eq. (6) results in

$$X_{11}(t)=\int_0^t\int_0^t\Big[\frac{\tilde{D}_1^2}{n^2}<\frac{\partial\beta(\boldsymbol{\xi})}{\partial\xi_1}\Big|_{\ell_1}\frac{\partial\beta(\boldsymbol{\zeta})}{\partial\zeta_1}\Big|_{\ell_2}+\frac{\tilde{D}_1}{n}<\frac{\partial\beta(\boldsymbol{\xi})}{\partial\xi_1}\Big|_{\ell_1}v_1(\boldsymbol{\zeta})\Big|_{\ell_2}>$$

$$+\frac{\tilde{D}_1}{n}<v_1(\boldsymbol{\xi})\Big|_{\ell_1}\frac{\partial\beta(\boldsymbol{\zeta})}{\partial\zeta_1}\Big|_{\ell_2}>+<v_1(\boldsymbol{\xi})\Big|_{\ell_1}v_1(\boldsymbol{\zeta})\Big|_{\ell_2}>\Big]ds_1ds_2, \tag{9}$$

where $\boldsymbol{\xi}=(\xi_1,\xi_2)$, $\boldsymbol{\zeta}=(\zeta_1,\zeta_2)$, $\ell_1=(<\tilde{v}_1>s_1,0)$, and $\ell_2=(<\tilde{v}_1>s_2,0)$. To arrive at Eq. (9), the solute particle was assumed to begin its motion at location $x_1=0$ and time $t=0$.

To proceed with the evaluation of solute displacement in the x_1 direction, the following section develops the statistics of the flow fields in Eq. (9) for the case where both the variations in hydraulic conductivity and the thickness of the confined aquifer are considered to be second-order stationary processes and the random processes of hydraulic conductivity and aquifer thickness are statistically independent.

3 Statistics of the flow fields

Chang et al. (2021) develop the differential equations for the flow fields (Eqs. (6) and (12) of Chang et al., 2021) in a confined aquifer with variable thickness based on a hydraulic approach to flow in aquifers (Bear, 1979; Bear and Cheng, 2010). On this basis, under the condition of steady-state flow, the equation for the depth-averaged specific discharge about the mean, keeping only first-order terms in the perturbations, take the following form

$$q_i = \bar{q}[(y+\beta)\delta_{1i} - \frac{1}{J}\frac{\partial h}{\partial x_i}] \qquad i=1,2, \tag{10a}$$

where $h = \tilde{h} - <\tilde{h}>$, $\tilde{h}$ is the depth-averaged hydraulic head, $J = -d<\tilde{h}>/dx_1$ (= constant), y = ln$K$-Y, K is the hydraulic conductivity, Y = <ln$K$>, $q_i = \tilde{q}_i - <\tilde{q}_i>$, $\bar{q} = <\tilde{q}_1> = e^Y J$, and the equation describing the depth-averaged head perturbation is of the form

$$\frac{\partial^2 h}{\partial x_i^2} = J[\frac{\partial y}{\partial x_1} + 2\frac{\partial \beta}{\partial x_1}] \qquad i=1,2. \tag{10b}$$

Equation (10) shows that the variations in log-hydraulic conductivity and log-aquifer thickness appear as forcing terms that produce the variations in depth-averaged head and hence the variations in depth-averaged specific discharge.

It follows from Eq. (10) that the terms for the statistics of the flow fields in Eq. (9), such as the covariance function for the log-aquifer thickness gradient, the cross-correlation between the log-aquifer thickness gradient and the depth-averaged flow velocity, and the covariance function for the depth-averaged flow velocity process, can be evaluated using the spectral representation theorem as follows:

$$<\frac{\partial \beta(\xi)}{\partial \xi_1}\frac{\partial \beta(\zeta)}{\partial \zeta_1}> = \frac{\partial^2}{\partial \xi_1 \partial \zeta_1} C_{\beta\beta}(\xi,\zeta), \tag{11}$$

$$<\frac{\partial \beta(\xi)}{\partial \xi_1} v_1(\zeta)> = VJ\frac{\partial}{\partial \xi_1} C_{\beta\beta}(\zeta,\xi) - V\frac{\partial^2}{\partial \xi_1 \partial \zeta_1} C_{\beta h_\beta}(\xi,\zeta), \tag{12a}$$

$$<v_1(\xi)\frac{\partial \beta(\zeta)}{\partial \zeta_1}> = VJ\frac{\partial}{\partial \zeta_1} C_{\beta\beta}(\xi,\zeta) - V\frac{\partial^2}{\partial \xi_1 \partial \zeta_1} C_{\beta h_\beta}(\zeta,\xi), \tag{12b}$$

$$\frac{<v_i(\xi)v_j(\zeta)>}{V^2} = [C_{yy}(\xi,\zeta) + C_{\beta\beta}(\xi,\zeta)]\delta_{1i}\delta_{1j} - \frac{1}{J}\frac{\partial}{\partial \zeta_j}[C_{yh_y}(\xi,\zeta) + C_{\beta h_\beta}(\xi,\zeta)]\delta_{1i}$$

$$-\frac{1}{J}\frac{\partial}{\partial \xi_i}[C_{yh_y}(\zeta,\xi) + C_{\beta h_\beta}(\zeta,\xi)]\delta_{1j} - -\frac{1}{J^2}\frac{\partial \gamma_h(\xi,\zeta)}{\partial \xi_i \partial \zeta_j}, \tag{13}$$

where $V=\overline{q}/n=e^{Y}J/n$, C_{yy} and $C_{\beta\beta}$ are the ln$K$ and ln$B$ covariance functions, respectively, C_{yh_y} is the covariance of ln$K$ process with the head process, $C_{\beta h_\beta}$ is the covariance of ln$B$ process with the head process, and γ_h is the semivariogram of the head process, defined as

$$\gamma_h(\xi,\zeta)=\gamma_{h_y}(\xi,\zeta)+\gamma_{h_\beta}(\xi,\zeta)=\frac{1}{2}\left\{<[h_y(\xi)-h_y(\zeta)]^2>+<[h_\beta(\xi)-h_\beta(\zeta)]^2>\right\}. \quad (14)$$

Note that C_{yh_y}, $C_{\beta h_\beta}$, and γ_h in Eqs. (12) and (13) can be calculated using the representation theorem for the depth-averaged head perturbation h (the perturbation solution of equation (10b)).

4 Results and discussion

To simplify the analysis of the variation of log-aquifer thickness on the variability of the solute displacement, this study considers the case where the local dispersivity is very small compared to the integral scales for the ln$K$ and ln$B$ processes, so that the solute dispersion is mainly caused by the spatial variability of hydraulic conductivity and thickness of confined aquifer. That is, solute dispersion occurs in situations where advection dominates and solute particles do not transfer across streamlines. Therefore, Eq. (9) can be simplified to

$$X_{11}(t)=\int_0^t\int_0^t < v_1(\xi)\Big|_{\ell_1} v_1(\zeta)\Big|_{\ell_2} > ds_1 ds_2 \cdot \tag{15}$$

That is, the variance of the solute displacement in the mean flow direction can only be determined with Eqs. (15) and (13). There are numerous studies in the literature on solute transport under advection-dominated conditions, e.g., Dagan (1984), Rubin and Bellin (1994), Butera et al. (2009), Cvetkovic (2016), Ciriello and Barros (2020), etc.

To determine the covariance function of the depth-averaged flow velocity, and thus the variance of solute displacement, it is assumed that the hydraulic conductivity and the thickness of the aquifer fields are lognormally distributed and characterized by the isotropic exponential covariance, i.e. (e.g., Dagan, 1984; Gelhar, 1993; Bailey and Baù, 2012)

$$C_{yy}(\xi,\zeta)=\sigma_y^2\exp[-\frac{|\xi-\zeta|}{\lambda_y}], \tag{16a}$$

$$C_{\beta\beta}(\xi,\zeta)=\sigma_\beta^2\exp[-\frac{|\xi-\zeta|}{\lambda_\beta}], \tag{16b}$$

where σ_y^2 and σ_β^2 are the variances of y and β, respectively, λ_y and λ_β are the integral scales of ln$K$ and ln$B$ fields, respectively. The corresponding spectra, which result from the inverse Fourier transform of Eq. (16), are as follows:

$$S_{yy}(R_1,R_2)=\frac{\sigma_y^2}{2\pi}\frac{\lambda_y^2}{[1+\lambda_y^2(R_1^2+R_2^2)]^{3/2}}, \tag{17a}$$

$$S_{\beta\beta}(R_1,R_2)=\frac{\sigma_\beta^2}{2\pi}\frac{\lambda_\beta^2}{[1+\lambda_\beta^2(R_1^2+R_2^2)]^{3/2}}. \tag{17b}$$

4.1 Covariance of flow velocity in the x_1-direction

Once the spectrum forms of the ln$K$ and ln$B$ fields are selected, the cross-correlation between the ln$K$ perturbation and the perturbation in the depth-averaged head, C_{yh_y}, the cross-correlation between the ln$B$ perturbation and the perturbation in the depth-averaged head, $C_{\beta h_\beta}$, and the semivariogram of the depth-averaged process, γ_h, can be determined as follows:

$$C_{yh_y}(\xi,\zeta)=\sigma_y^2\lambda_y J\Big[\Theta_1(\frac{\xi_1}{\lambda_y},\frac{\xi_2}{\lambda_y})-\frac{\zeta_1}{\lambda_y}\Theta_2(\frac{\xi_1}{\lambda_y},\frac{\xi_2}{\lambda_y})+\frac{\zeta_2}{\lambda_y}\Theta_3(\frac{\xi_1}{\lambda_y},\frac{\xi_2}{\lambda_y})-\Theta_1(\frac{\rho_1}{\lambda_y},\frac{\rho_2}{\lambda_y})\Big], \tag{18}$$

$$C_{\beta h_\beta}(\xi,\zeta)=2\sigma_y^2\lambda_\beta J\Big[\Theta_1(\frac{\xi_1}{\lambda_\beta},\frac{\xi_2}{\lambda_\beta})-\frac{\zeta_1}{\lambda_\beta}\Theta_2(\frac{\xi_1}{\lambda_\beta},\frac{\xi_2}{\lambda_\beta})+\frac{\zeta_2}{\lambda_\beta}\Theta_3(\frac{\xi_1}{\lambda_\beta},\frac{\xi_2}{\lambda_\beta})-\Theta_1(\frac{\rho_1}{\lambda_\beta},\frac{\rho_2}{\lambda_\beta})\Big], \tag{19}$$

$$\gamma_h(\xi,\zeta)=\gamma_{h_y}(\xi,\zeta)+\gamma_{h_\beta}(\xi,\zeta), \tag{20a}$$

$$\gamma_{h_y}(\xi,\zeta)=\frac{1}{2}\sigma_y^2\lambda_y^2J^2\Big\{\frac{3}{8}\frac{\rho_1^2}{\lambda_y^2}+\frac{1}{8}\frac{\rho_2^2}{\lambda_y^2}+\Psi_1(\frac{\rho_1}{\lambda_y},\frac{\rho_2}{\lambda_y})+\frac{\rho_1}{\lambda_y}[-\frac{\xi_1}{\lambda_y}\Psi_2(\frac{\xi_1}{\lambda_y},\frac{\xi_2}{\lambda_y})+\frac{\zeta_1}{\lambda_y}\Psi_2(\frac{\zeta_1}{\lambda_y},\frac{\zeta_2}{\lambda_y})]$$
$$+\frac{\rho_2}{\lambda_y}[\frac{\xi_2}{\lambda_y}\Psi_3(\frac{\xi_1}{\lambda_y},\frac{\xi_2}{\lambda_y})-\frac{\zeta_2}{\lambda_y}\Psi_3(\frac{\zeta_1}{\lambda_y},\frac{\zeta_2}{\lambda_y})]\Big\}, \tag{20b}$$

$$\gamma_{h_\beta}(\xi,\zeta)=2\sigma_\beta^2\lambda_\beta^2J^2\Big\{\frac{3}{8}\frac{\rho_1^2}{\lambda_\beta^2}+\frac{1}{8}\frac{\rho_2^2}{\lambda_\beta^2}+\Psi_1(\frac{\rho_1}{\lambda_\beta},\frac{\rho_2}{\lambda_\beta})+\frac{\rho_1}{\lambda_\beta}[-\frac{\xi_1}{\lambda_\beta}\Psi_2(\frac{\xi_1}{\lambda_\beta},\frac{\xi_2}{\lambda_\beta})+\frac{\zeta_1}{\lambda_\beta}\Psi_2(\frac{\zeta_1}{\lambda_\beta},\frac{\zeta_2}{\lambda_\beta})]$$
$$+\frac{\rho_2}{\lambda_\beta}[\frac{\xi_2}{\lambda_\beta}\Psi_3(\frac{\xi_1}{\lambda_\beta},\frac{\xi_2}{\lambda_\beta})-\frac{\zeta_2}{\lambda_\beta}\Psi_3(\frac{\zeta_1}{\lambda_\beta},\frac{\zeta_2}{\lambda_\beta})]\Big\}, \tag{20c}$$

where $\rho_1 = \xi_1$-ζ_1, $\rho_2 = \xi_2$-ζ_2, and the description of functions Θ_1 through Θ_3, or Ψ_1 through Ψ_3, can be found in Appendix B. Detailed derivations of Eq. (18) to Eq. (20) can be found in Appendix B.

In the case of statistically nonhomogeneous random fields, the structure of variability can be characterized by considering the semivariogram of a random field. If the semivariogram depends only on the separation, the random field is said to have stationary increments. The semivariogram in Eq. (20) clearly depends on the spatial location, which means that the processes of depth-averaged hydraulic head are nonstationary.

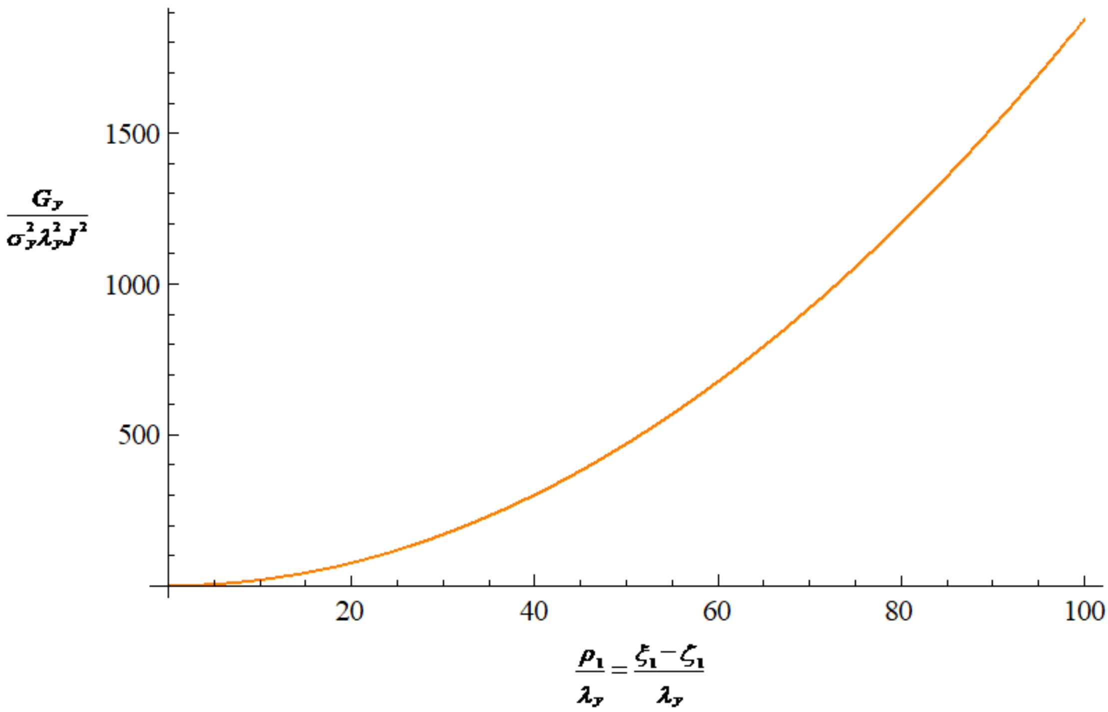

Figure 1. The stationary parts of the semivariogram of the head field, reflecting the effect of variation in the hydraulic conductivity fields, as a function of the separation distance in the mean flow direction, where G_y is the sum of the first three terms on the right-hand side of Eq. (20b).

Figure 1 shows graphically the behavior of the stationary parts of the semivariogram (namely, the sum of the first three terms on the right-hand side of Eq. (20b)) as a function of the separation distance in the x_1-direction (mean flow direction).

The semivariogram of the head field, reflecting the effect of variation in the hydraulic conductivity fields, shows an unlimited increase, as shown in Fig. 1. The unbounded head semivariogram suggests that there is no head covariance function (or the hydraulic head field with infinite variance). When taking samples from a field, one obtains a histogram from which a certain value of the variance can always be calculated. However, for many phenomena, the experimental variance is actually a function of the field. In particular, it increases as the field increases, i.e., many phenomena have an almost unlimited capacity of dispersion and cannot be adequately described by ascribing to them a finite a priori variance. In this case, the use of the semivariogram is an appropriate way to measure the variability of the variation. Similar conclusions can be drawn from Fig. 2, a graphical representation of the stationary parts of the semivariogram of the head field in Eq. (20c) in the mean flow direction, which reflects the effect of the variation of the aquifer thickness fields.

At this point, the covariance function for the depth-averaged velocity process in Eq. (13) can now be determined in conjunction with Eqs. (16), and (18)-(20). For example, the covariance of flow velocity for the separation along the mean flow direction is explicitly determined as follows:

$$< v_1(\xi_1,\xi_2) v_1(\zeta_1,\zeta_2=\xi_2) > = < v_{y_1}(\xi_1,\xi_2) v_{y_1}(\zeta_1,\xi_2) > + < v_{\beta_1}(\xi_1,\xi_2) v_{\beta_1}(\zeta_1,\xi_2) >, \qquad (21a)$$

where

$$\frac{<v_{y_1}(\xi_1,\xi_2)v_{y_1}(\zeta_1,\xi_2)>}{V^2}=\sigma_y^2\Big\{\frac{3}{8}+\exp(-\frac{\rho}{\lambda_y})-\Big[2\Xi_1(\frac{\rho_1}{\lambda_y},0)-\Xi_1(\frac{\xi_1}{\lambda_y},\frac{\xi_2}{\lambda_y})-\Xi_1(\frac{\zeta_1}{\lambda_y},\frac{\xi_2}{\lambda_y})\Big]$$

$$+\Big[\Xi_2(\frac{\rho_1}{\lambda_y},0)-\Xi_2(\frac{\xi_1}{\lambda_y},\frac{\xi_2}{\lambda_y})-\Xi_2(\frac{\zeta_1}{\lambda_y},\frac{\xi_2}{\lambda_y})\Big]\Big\}, \qquad (21b)$$

$$\frac{<v_{\beta_1}(\xi_1,\xi_2)v_{\beta_1}(\zeta_1,\xi_2)>}{V^2}=\sigma_\beta^2\Big\{\frac{3}{2}+\exp(-\frac{\rho}{\lambda_\beta})-2\Big[2\Xi_1(\frac{\rho_1}{\lambda_\beta},0)-\Xi_1(\frac{\xi_1}{\lambda_\beta},\frac{\xi_2}{\lambda_\beta})-\Xi_1(\frac{\zeta_1}{\lambda_\beta},\frac{\xi_2}{\lambda_\beta})\Big]$$

$$+4\Big[\Xi_2(\frac{\rho_1}{\lambda_\beta},0)-\Xi_2(\frac{\xi_1}{\lambda_\beta},\frac{\xi_2}{\lambda_\beta})-\Xi_2(\frac{\zeta_1}{\lambda_\beta},\frac{\xi_2}{\lambda_\beta})\Big]\Big\}, \qquad (21c)$$

$\rho=(\rho_1^2+\rho_2^2)^{1/2}$ and expressions for Ξ_1 and Ξ_2 are given, respectively, in the Appendix C. This should be used to compute the variance of solute displacement in the mean flow direction. The nonstationarity of the velocity covariance in Eq. (21) is evident in the dependence on spatial location, which is caused by nonstationarity in the hydraulic head processes.

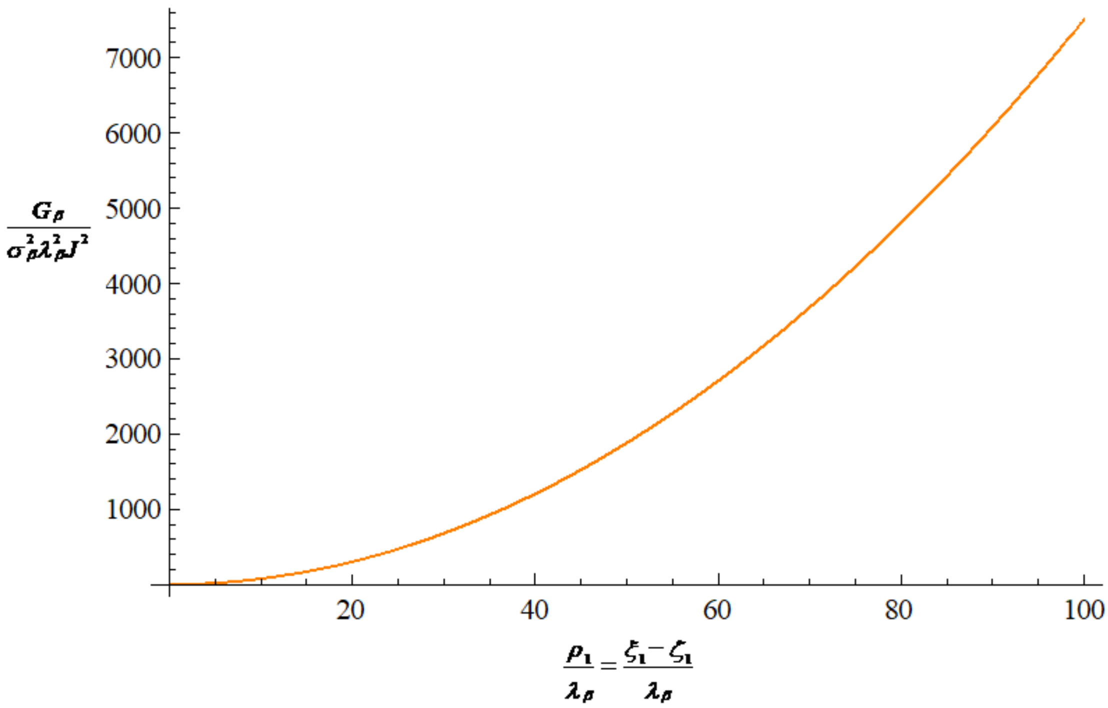

Figure 2. The stationary parts of the semivariogram of the head field, reflecting the effect of the variation of the aquifer thickness fields, as a function of the separation

distance in the mean flow direction, where G_β is the sum of the first three terms on the right-hand side of Eq. (21c).

In the limit of $\zeta_1 \rightarrow \xi_1$, Eq. (21) approaches to the velocity variances in the mean flow direction as

$$\sigma_v^2 = \sigma^2_{v_y}(\xi_1, \xi_2) + \sigma^2_{v_\beta}(\xi_1, \xi_2), \tag{22a}$$

where

$$\frac{\sigma^2_{v_y}}{V^2\sigma_y^2} = \frac{1}{4}\frac{1}{\xi^8}\Delta_1\left(\frac{\xi_1}{\lambda_y}, \frac{\xi_2}{\lambda_y}\right) + \frac{1}{4}\frac{1}{\xi^9}\exp\left[-\frac{\xi}{\lambda_y}\right]\Delta_2\left(\frac{\xi_1}{\lambda_y}, \frac{\xi_2}{\lambda_y}\right), \tag{22b}$$

$$\frac{\sigma^2_{v_\beta}}{V^2\sigma_\beta^2} = \frac{1}{2}\frac{1}{\xi^8}\Delta_3\left(\frac{\xi_1}{\lambda_\beta}, \frac{\xi_2}{\lambda_y}\right) + \frac{1}{2}\frac{1}{\xi^9}\exp\left[-\frac{\xi}{\lambda_\beta}\right]\Delta_4\left(\frac{\xi_1}{\lambda_\beta}, \frac{\xi_2}{\lambda_\beta}\right), \tag{22c}$$

$\xi = (\xi_1^2+\xi_2^2)^{1/2}$ and expressions for Δ_1-Δ_4 are given, respectively, in the Appendix D. From Eq. (22), it can be seen that the variance of the flow velocity is positively correlated with the variances of the log-hydraulic conductivity and log-aquifer thickness. This means that the variability of the flow velocity field increases with the variability of the hydraulic conductivity and aquifer thickness fields.

4.2 Variance of the solute displacement in the mean flow direction

4.2.1 Nonstationary flow fields

Substituting Eq. (21) into Eq. (15) and integrating it yields the following expression for the variance of longitudinal solute displacement as

$$X_{11}(t) = X_{11_y}(t) + X_{11_\beta}(t)\,, \tag{23a}$$

where

$$\frac{X_{11_y}(t)}{\sigma_y^2 \lambda_y^2} = \frac{5}{2} - 3\gamma - \frac{9}{\Gamma^2} + 2\Gamma + \frac{3}{8}\Gamma^2 + 3Ei(-\Gamma) - 3\ln(\Gamma) + e^{-\Gamma}\left(2 + \frac{9}{\Gamma^2} + \frac{9}{\Gamma}\right), \tag{23b}$$

$$\frac{X_{11_\beta}(t)}{\sigma_\beta^2 \lambda_\beta^2} = 4 - 4\gamma - \frac{36}{\vartheta^2} + 2\vartheta + \frac{3}{2}\vartheta^2 + 4Ei(-\vartheta) - 4\ln(\vartheta) + 2e^{-\vartheta}\left(7 + 2\vartheta + \frac{18}{\vartheta^2} + \frac{18}{\vartheta}\right), \tag{23c}$$

$\Gamma = Vt/\lambda_y$, and $\vartheta = Vt/\lambda_\beta$.

4.2.2 Stationary flow fields

Gutjahr and Gelhar (1981) show that the Poission equation in an unbounded porous medium such as equation (B1a) also has a zero-order intrinsic random function (0-IRF) as its solution when the input random process has a finite variance. That is, Eqs. (B1a) and (B1b) with stationary processes y and β admit the solutions of the form

$$h_y(x_1, x_2) = J \int_{-\infty}^{\infty}\int_{-\infty}^{\infty} iR_1 \frac{1 - \exp[i(R_1 x_1 + R_2 x_2)]}{R_1^2 + R_2^2} dZ_y(R_1, R_2)\,, \tag{24a}$$

$$h_\beta(x_1, x_2) = 2J \int_{-\infty}^{\infty}\int_{-\infty}^{\infty} iR_1 \frac{1 - \exp[i(R_1 x_1 + R_2 x_2)]}{R_1^2 + R_2^2} dZ_\beta(R_1, R_2)\,. \tag{24b}$$

Using a similar methodology as above and based on Eq. (24), one would arrive at the following results

$$C_{yh_y}(\xi,\zeta)=\sigma_y^2\lambda_y J\left[\Theta_1\left(\frac{\xi_1}{\lambda_y},\frac{\xi_2}{\lambda_y}\right)-\Theta_1\left(\frac{\rho_1}{\lambda_y},\frac{\rho_2}{\lambda_y}\right)\right], \tag{25a}$$

$$C_{yh_y}(\xi,\zeta)=\sigma_y^2\lambda_y J\left[\Theta_1\left(\frac{\xi_1}{\lambda_y},\frac{\xi_2}{\lambda_y}\right)-\Theta_1\left(\frac{\rho_1}{\lambda_y},\frac{\rho_2}{\lambda_y}\right)\right], \tag{25b}$$

$$\gamma_{h_y}(\xi,\zeta)=\frac{1}{2}\sigma_y^2\lambda_y^2 J^2\Psi_1\left(\frac{\rho_1}{\lambda_y},\frac{\rho_2}{\lambda_y}\right), \tag{26a}$$

$$\gamma_{h_\beta}(\xi,\zeta)=2\sigma_\beta^2\lambda_\beta^2 J^2\Psi_1\left(\frac{\rho_1}{\lambda_\beta},\frac{\rho_2}{\lambda_\beta}\right), \tag{26b}$$

from which it follows that in the mean flow direction,

$$<v_1(\xi_1,\xi_2)v_1(\zeta_1,\zeta_2=\xi_2)>=<v_{y_1}(\xi_1,\xi_2)v_{y_1}(\zeta_1,\xi_2)>+<v_{\beta_1}(\xi_1,\xi_2)v_{\beta_1}(\zeta_1,\xi_2)>, \tag{27a}$$

where

$$\frac{<v_{y_1}(\xi_1,\xi_2)v_{y_1}(\zeta_1,\xi_2)>}{V^2}=\sigma_y^2\left[\frac{3}{2}\left(-\frac{6}{\varphi^4}+\frac{1}{\varphi^2}\right)+3e^{-\varphi}\left(\frac{3}{\varphi^4}+\frac{3}{\varphi^3}+\frac{1}{\varphi^2}\right)\right], \tag{27b}$$

$$\frac{<v_{\beta_1}(\xi_1,\xi_2)v_{\beta_1}(\zeta_1,\xi_2)>}{V^2}=\sigma_\beta^2\left[-2\left(\frac{18}{\upsilon^4}+\frac{1}{\upsilon^2}\right)+e^{-\varphi}\left(1+\frac{36}{\upsilon^4}+\frac{36}{\upsilon^3}+\frac{16}{\upsilon^2}+\frac{4}{\upsilon}\right)\right], \tag{27c}$$

$\varphi = (\xi_1\text{-}\zeta_1)/\lambda_y$ and $\upsilon = (\xi_1\text{-}\zeta_1)/\lambda_\beta$. Finally, the variance of solute displacement in the mean flow direction is obtained from Eq. (15) by applying Eq. (27):

$$X_{11}(t)=X_{11_y}(t)+X_{11_\beta}(t), \tag{28a}$$

where

$$\frac{X_{11_y}(t)}{\sigma_y^2\lambda_y^2}=\frac{3}{2}-3\gamma+2\Gamma-\frac{3}{\Gamma^2}+3Ei(-\Gamma)-3\ln(\Gamma)+3e^{-\Gamma}\left(\frac{1}{\Gamma^2}+\frac{1}{\Gamma}\right), \tag{28b}$$

$$\frac{X_{11_\beta}(t)}{\sigma_\beta^2\lambda_\beta^2}=4-4\gamma-\frac{12}{\vartheta^2}+2\vartheta+4Ei(-\vartheta)-4\ln(\vartheta)+2e^{-\vartheta}\left(1+\frac{6}{\vartheta^2}+\frac{6}{\vartheta}\right). \tag{28c}$$

Equation (28b) is equivalent to the solution of Dagan (1982; 1984) using the Green function approach, where the variance and integral scale of the log conductivity fields in Eq. (28b) are replaced by the variance and integral scale of the log transmissivity fields.

A comparison of the prediction of the solute longitudinal displacement variance in Eq. (23b) in nonstationary flow fields with the prediction in Eq. (28b) in stationary flow fields is shown graphically in Fig. 3. The variance of the longitudinal displacement in response to the change in the hydraulic conductivity grows monotonically with travel time. It can also be seen that the difference in displacement variance caused by the nonstationary and stationary flow fields increases with travel time, which means that the longitudinal mscrodispersion in nonstationary flow fields becomes anomalous and a Fick’s regime is not achieved. This behavior of anomalous macrodispersion is attributed to the effect of nonstationary hydraulic head fields caused by the variation of hydraulic conductivity.

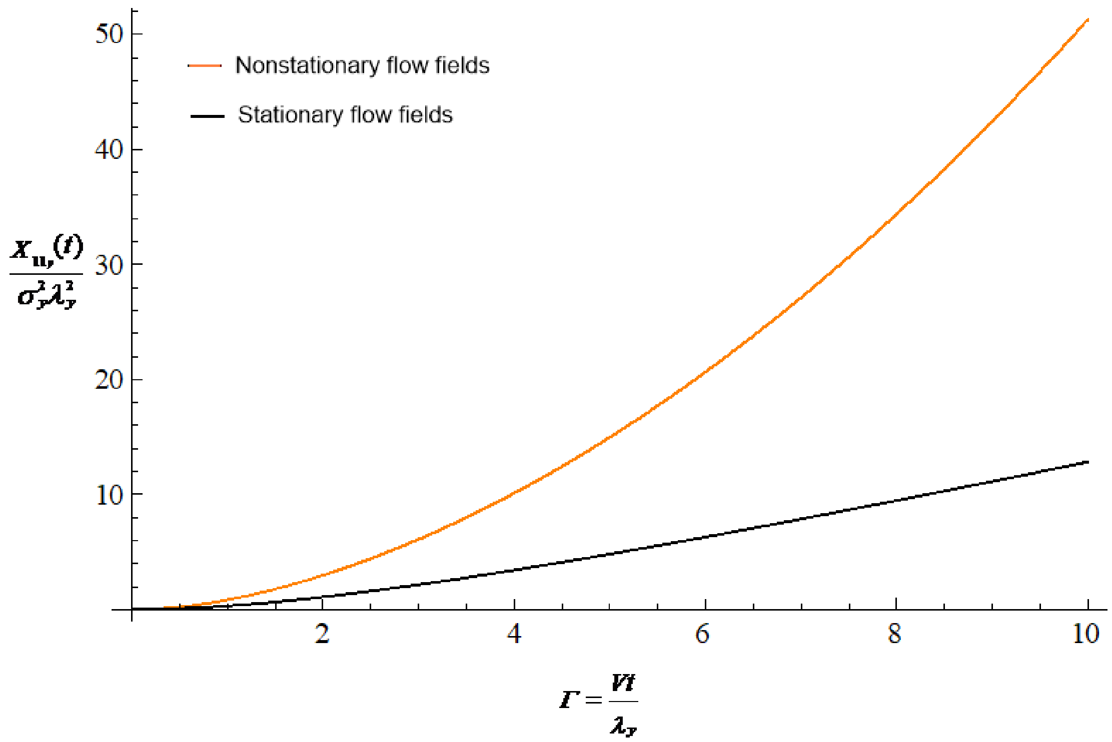

Figure 3. Comparison of the prediction of the solute longitudinal displacement variance in Eq. (23b) in nonstationary flow fields with the prediction in Eq. (28b) in stationary flow fields.

A macrodispersion coefficient in the mean flow direction can be defined by half of the time derivative of Eq. (23b) as follows:

$$D_{11_y}(t) = \sigma_y^2 \lambda_y V\left[1 + \frac{9}{\Gamma^3} - \frac{3}{2}\frac{1}{\Gamma} + \frac{3}{8}\Gamma - e^{-\Gamma}\left(1 + \frac{9}{\Gamma^3} + \frac{9}{\Gamma^2} + \frac{3}{\Gamma}\right)\right]. \tag{29a}$$

This implies that the longitudinal macrodispersion coefficient at large time in nonstationary flow fields can be approximated as

$$D_{11_y}(t) \approx \sigma_y^2 \lambda_y V\left(1 + \frac{3}{8}\Gamma\right). \tag{29b}$$

That is, the longitudinal macrodispersion increases linearly with travel time at large distances. Note that, in stationary flow fields, the longitudinal macrodispersion coefficient approaches an asymptotic limit D_{11_y} = $\sigma_y^2 \lambda_y V$ at large time. Clearly, applying the asymptotic macrodispersion coefficient (Eq. (29b)), which is appropriate for macrodispersion in stationary flow fields, to the prediction of macrodispersion in the downstream region at a large distance from the contamination source leads to a significant underestimation of macrodispersion in nonstationary flow fields.

The behavior of the longitudinal displacement variance of solutes, affected by the effect of variation of aquifer thickness field, in the nonstationary flow field (Eq. (23c)) and in the stationary flow field (Eq. (28c)) as a function of travel time is also presented graphically in Fig. 4. This again demonstrates that the displacement variance grows faster than linear with travel time and the longitudinal macrodispersion becomes anomalous at large travel times. The corresponding longitudinal macrodispersion coefficient is

$$D_{11_\beta}(t)=\sigma_\beta^2\lambda_\beta V\Big[1+\frac{36}{\vartheta^3}-\frac{2}{\vartheta}+\frac{3}{2}\vartheta-e^{-\vartheta}\Big(5+\frac{36}{\vartheta^3}+\frac{36}{\vartheta^2}+\frac{16}{\vartheta}+2\vartheta\Big)\Big], \tag{30a}$$

with the approximation at large times as

$$D_{11_\beta}(t)\approx\sigma_\beta^2\lambda_\beta V\Big(1+\frac{3}{2}\vartheta\Big). \tag{30b}$$

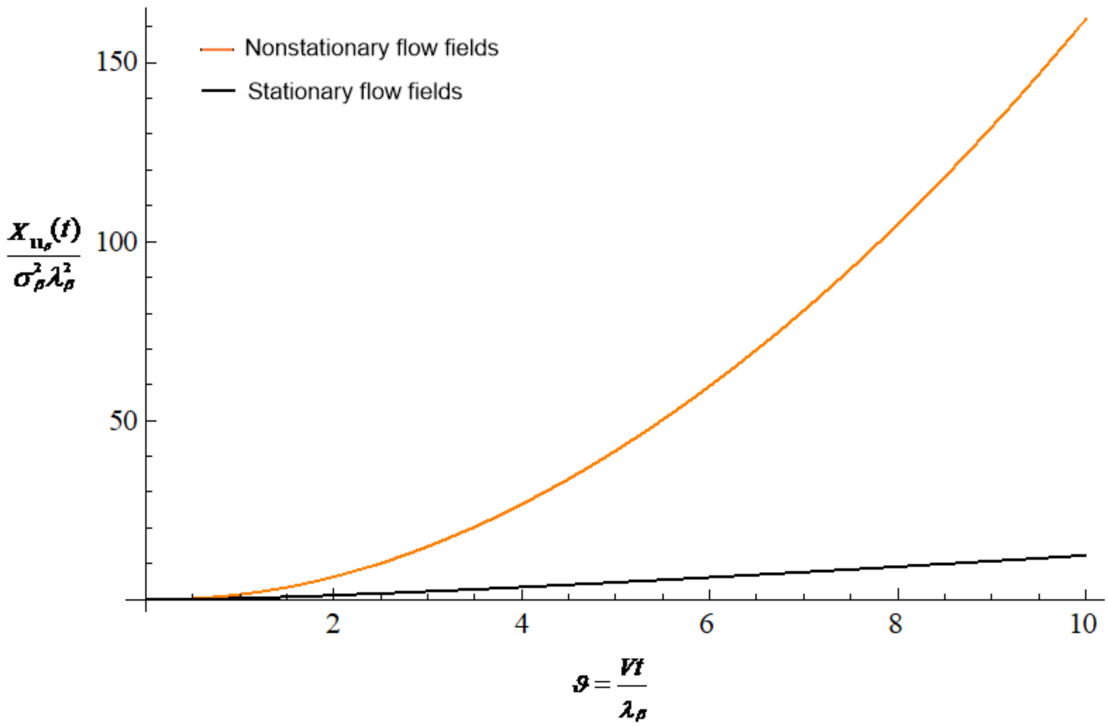

Figure 4. Comparison of the prediction of the solute longitudinal displacement variance in Eq. (23c) in nonstationary flow fields with the prediction in Eq. (28c) in stationary flow fields.

5 Conclusions

In this work, a theoretical stochastic methodology is developed to quantify the displacement variance of an inert solute particle in heterogeneous confined aquifers with variable thickness. This methodology relates solute displacement to the Fokker-Planck equation through the two-dimensional depth-averaged solute mass conservation equation. In contrast to previous stochastic studies of two-dimensional solute transport problems, the variability of solute movement is caused not only by the variability of log conductivity, but also by the variability of log thickness of confined aquifer.

The two-dimensional stochastic groundwater flow equation for the depth-averaged hydraulic head perturbation always has a 1-IRF solution when the log hydraulic conductivity and log aquifer thickness fields are second-order stationary. This leads to an unbounded increasing head semivariogram where no head covariance exists. The nonstationarity of the hydraulic head leads to nonstationary flow velocity fields and thus a nonlinear increase in longitudinal solute displacement with travel time. That is, a Fick's regime is not achieved, and the longitudinal macrodispersion becomes anomalous and increases linearly with travel time at large distances. It is also shown that the variability of solute displacement in the mean flow direction increases with the variability of hydraulic conductivity and aquifer thickness.

Appendix A: Development of Eq. (2)

When the dispersion tensor is expressed in its three principal directions and these principal directions are used as Cartesian coordinate axes, the equation for the transport of inert solutes through a rigid, saturated porous medium is (e.g., de Marsily, 1986)

$$n\frac{\partial c}{\partial t}=\frac{\partial}{\partial x_i}[D_i\frac{\partial c}{\partial x_i}-cq_i] \qquad i=1,2,3, \qquad \text{(A1)}$$

where n is the porosity, c is the solute concentration, and D_i and q_i are the dispersion coefficient and the specific discharge in the x_i direction, respectively. Integrating Eq. (A1) with respect to x_3 over the vertical thickness of a confined aquifer, $B(x_1, x_2)$, together with Leibniz's rule and no-slip condition for the dispersive and diffusive fluxes at upper and lower boundaries of the confined aquifer, yields the two-dimensional, depth-averaged equation for conservation of solute mass (e.g., Holly, 1975; Fischer et al., 1979)

$$\frac{\partial}{\partial t}[B\tilde{c}]=\frac{\partial}{\partial x_i}[\frac{\tilde{D}_i}{n}B\frac{\partial \tilde{c}}{\partial x_i}]-\frac{\partial}{\partial x_i}[\frac{\tilde{q}_i}{n}B\tilde{c}] \qquad i=1,2, \qquad \text{(A2)}$$

where $\tilde{D}_i$, $\tilde{c}$, and $\tilde{q}_i$ represent the depth-averaged dispersion coefficient, depth-averaged solute concentration, and depth-averaged specific discharge, respectively. Note that in developing Eq. (A2), it is assumed that the contaminant plume in confined aquifers is well mixed over depth, so that variations around the depth-averaged concentration are relatively small (Holly, 1975). Then the average of the product of concentration and velocity fluctuations can be assumed to be absorbed in the gradient transport terms in Eq. (A2)

Starting from the identity,

$$\frac{\tilde{D}_i}{n}B\frac{\partial \tilde{c}}{\partial x_i}=\frac{\partial}{\partial x_i}[\frac{\tilde{D}_i}{n}B\tilde{c}]-\tilde{c}\frac{\partial}{\partial x_i}[\frac{\tilde{D}_i}{n}B]$$

$$=\frac{\partial}{\partial x_i}[\frac{\tilde{D}_i}{n}B\tilde{c}]-B\tilde{c}\frac{1}{n}\frac{\partial \tilde{D}_i}{\partial x_i}-\frac{\tilde{D}_i}{n}B\tilde{c}\frac{\partial \ln B}{\partial x_i} \qquad i=1,2, \qquad \text{(A3)}$$

Eq. (A2) can be rewritten as follows:

$$\frac{\partial}{\partial t}[B\tilde{c}]=\frac{\partial^2}{\partial x_i^2}[\frac{\tilde{D}_i}{n}B\tilde{c}]-\frac{\partial}{\partial x_i}[(\frac{1}{n}\frac{\partial \tilde{D}_i}{\partial x_i}+\frac{\tilde{D}_i}{n}\frac{\partial \ln B}{\partial x_i}+\frac{\tilde{q}_i}{n})B\tilde{c}] \qquad i=1,2, \tag{A4}$$

which corresponds to the form of the Fokker-Planck equation (e.g., Risken, 1989).

The concentration field associated with the solute particle can be written as (Fischer et al., 1979; Dagan, 1989)

$$B\tilde{c}=\frac{M}{n}f(\boldsymbol{x};t,\boldsymbol{a},t_0), \tag{A5}$$

where M is the solute mass, $f(\boldsymbol{x};t,\boldsymbol{a},t_0)$ stands for the probability density function of the particle displacement which originates at $\boldsymbol{x} = \boldsymbol{a}$ for $t = t_0$. Substituting Eq. (A5) into Eq. (A4) gives

$$\frac{\partial}{\partial t}f(\boldsymbol{x};t)=\frac{\partial^2}{\partial x_i^2}[\frac{\tilde{D}_i}{n}f(\boldsymbol{x};t)]-\frac{\partial}{\partial x_i}[(\frac{1}{n}\frac{\partial \tilde{D}_i}{\partial x_i}+\frac{\tilde{D}_i}{n}\frac{\partial \ln B}{\partial x_i}+\frac{\tilde{q}_i}{n})f(\boldsymbol{x};t)] \qquad i=1,2, \tag{A6}$$

which is known as the Fokker-Planck equation. Moreover, it can be shown that the stochastic differential equation for the evolution of stochastic process (e.g., Van Kampen, 1992; Jing et al., 2019)

$$\frac{dX_i}{dt}=\mu_i(\boldsymbol{X}(t))+\sigma_i(\boldsymbol{X}(t))\frac{dW}{dt} \qquad i=1,2, \tag{A7}$$

where $\boldsymbol{X}(= (X_1,X_2))$ is the displacement, μ_i is the drift coefficient, σ_i is the diffusion coefficient, and W denotes a Wiener process, is equivalent to the Fokker-Planck equation (A6) such that

$$\mu_i=\frac{1}{n}\frac{\partial}{\partial x_i}\tilde{D}_i(\boldsymbol{X})+\frac{1}{n}\tilde{D}_i(\boldsymbol{X})\frac{\partial}{\partial x_i}\ln B(\boldsymbol{X})+\frac{1}{n}\tilde{q}_i(\boldsymbol{X}) \qquad i=1,2, \tag{A8a}$$

$$\sigma_i^2=\frac{2}{n}\tilde{D}_i(\boldsymbol{X}) \qquad i=1,2, \tag{A8b}$$

Using Eq. (A8), Eq. (A7) leads to Eq. (2).

Appendix B: Derivations of Eq. (18) to Eq. (20)

Due to the property of the linearity of the driving forces, Eq. (10b) can alternatively be divided into two parts as

$$\frac{\partial^2 h_y}{\partial x_i^2} = J\frac{\partial y}{\partial x_1} \qquad i = 1,2, \tag{B1a}$$

$$\frac{\partial^2 h_\beta}{\partial x_i^2} = 2J\frac{\partial \beta}{\partial x_1} \qquad i = 1,2, \tag{B1b}$$

where $h = h_y + h_\beta$. Matheron (1973) shows that if the random input process of the Poission equation is second-order stationary, then the Poission equation has a first-order intrinsic random function (1-IRF) as its solution. Since the processes y and β are second-order stationary, it can be shown that the derivatives of the processes y and β with respect to x_1 are also stationary. This means that Eq. (B1) has a 1-IRF solution for h_y and h_β which admits the Fourier-Stieltjes representation as follows:

$$h_y(x_1, x_2) = J\int_{-\infty}^{\infty}\int_{-\infty}^{\infty} iR_1 \frac{1-\exp[i(R_1x_1+R_2x_2)]+i(R_1x_1+R_2x_2)}{R_1^2+R_2^2}\, dZ_y(R_1, R_2), \tag{B2a}$$

$$h_\beta(x_1, x_2) = 2J\int_{-\infty}^{\infty}\int_{-\infty}^{\infty} iR_1 \frac{1-\exp[i(R_1x_1+R_2x_2)]+i(R_1x_1+R_2x_2)}{R_1^2+R_2^2}\, dZ_\beta(R_1, R_2)\,. \tag{B2b}$$

where R_1 and R_2 are the components of the wave number vector $\boldsymbol{R}$ (= (R_1, R_2)), and Z_y

and Z_β are complex-valued distributions with uncorrelated increments on wave number space. Note that a 1-IRF is the second integral of a zero-mean spatial random function (Chile`s and Delfiner, 1999).

The stationarity of the ln$K$ process allows the Fourier-Stieltjes representations (e.g., Lumley and Panofsky, 1964)

$$y(x_1, x_2) = \int_{-\infty}^{\infty}\int_{-\infty}^{\infty} \exp[i(R_1 x_1 + R_2 x_2)] dZ_y(R_1, R_2). \tag{B3}$$

Using this and Eqs. (B2a) and (24a), the covariance of ln$K$ process with the head process C_{yh} in Eq. (12) is given as

$$C_{yh_y}(\xi, \zeta) = < y(\xi) h_y(\zeta) >$$

$$= -J \int_{-\infty}^{\infty}\int_{-\infty}^{\infty} i \frac{R_1}{R_1^2 + R_2^2} \exp[i(R_1\xi_1 + R_2\xi_2)] \{1 - \exp[-i(R_1\zeta_1 + R_2\zeta_2)] - i(R_1\zeta_1 + R_2\zeta_2)\}$$

$$\times \frac{\sigma_y^2}{2\pi} \frac{\lambda_y^2}{[1 + \lambda_y^2(R_1^2 + R_2^2)]^{3/2}} dR_1 dR_2$$

$$= \sigma_y^2 \lambda_y J [\Theta_1(\frac{\xi_1}{\lambda_y}, \frac{\xi_2}{\lambda_y}) - \frac{\zeta_1}{\lambda_y}\Theta_2(\frac{\xi_1}{\lambda_y}, \frac{\xi_2}{\lambda_y}) + \frac{\zeta_2}{\lambda_y}\Theta_3(\frac{\xi_1}{\lambda_y}, \frac{\xi_2}{\lambda_y}) - \Theta_1(\frac{\rho_1}{\lambda_y}, \frac{\rho_2}{\lambda_y})], \tag{B4}$$

where $\rho_1 = \xi_1 - \zeta_1$, $\rho_2 = \xi_2 - \zeta_2$, and

$$\Theta_1(a,b) = \frac{a}{r}[1 - e^{-r}(1+r)], \tag{B5a}$$

$$\Theta_2(a,b) = -2\frac{a^2}{r^4} + \frac{1}{r^2} + e^{-r}[a^2(\frac{2}{r^4} + \frac{2}{r^3} + \frac{1}{r^2}) - \frac{1}{r^2} - \frac{1}{r}], \tag{B5b}$$

$$\Theta_3(a,b) = ab[\frac{2}{r^4} - e^{-r}(\frac{2}{r^4} + \frac{2}{r^3} + \frac{1}{r^2})], \tag{B5c}$$

$r^2 = a^2 + b^2$.

Similarly, the closed-form expression for the covariance of ln$B$ process with the head process $C_{\beta h_\beta}$ in Eq. (12) can be obtained using Eqs. (B2b), (24b), and the Fourier-Stieltjes representations for the stationary ln$B$ process

$$\beta(x_1, x_2) = \int_{-\infty}^{\infty}\int_{-\infty}^{\infty} \exp[i(R_1 x_1 + R_2 x_2)] dZ_\beta(R_1, R_2), \tag{B6}$$

which is in the form

$$C_{\beta h_\beta}(\xi,\zeta) = <\beta(\xi) h_\beta(\zeta)>$$
$$= 2\sigma_y^2 \lambda_\beta J\left[\Theta_1(\frac{\xi_1}{\lambda_\beta},\frac{\xi_2}{\lambda_\beta}) - \frac{\zeta_1}{\lambda_\beta}\Theta_2(\frac{\xi_1}{\lambda_\beta},\frac{\xi_2}{\lambda_\beta}) + \frac{\zeta_2}{\lambda_\beta}\Theta_3(\frac{\xi_1}{\lambda_\beta},\frac{\xi_2}{\lambda_\beta}) - \Theta_1(\frac{\rho_1}{\lambda_\beta},\frac{\rho_2}{\lambda_\beta})\right]. \tag{B7}$$

Substituting Eq. (B2) into Eq. (13), it is found that the semivariogram of the head process has the following form

$$\gamma_{h_y}(\xi,\zeta) = \frac{1}{2}\sigma_y^2 \lambda_y^2 J^2 \{\frac{3}{8}\frac{\rho_1^2}{\lambda_y^2} + \frac{1}{8}\frac{\rho_2^2}{\lambda_y^2} + \Psi_1(\frac{\rho_1}{\lambda_y},\frac{\rho_2}{\lambda_y}) + \frac{\rho_1}{\lambda_y}[-\frac{\xi_1}{\lambda_y}\Psi_2(\frac{\xi_1}{\lambda_y},\frac{\xi_2}{\lambda_y}) + \frac{\zeta_1}{\lambda_y}\Psi_2(\frac{\zeta_1}{\lambda_y},\frac{\zeta_2}{\lambda_y})]$$
$$+ \frac{\rho_2}{\lambda_y}[\frac{\xi_2}{\lambda_y}\Psi_3(\frac{\xi_1}{\lambda_y},\frac{\xi_2}{\lambda_y}) - \frac{\zeta_2}{\lambda_y}\Psi_3(\frac{\zeta_1}{\lambda_y},\frac{\zeta_2}{\lambda_y})]\}, \tag{B8a}$$

$$\gamma_{h_\beta}(\xi,\zeta) = 2\sigma_\beta^2 \lambda_\beta^2 J^2 \{\frac{3}{8}\frac{\rho_1^2}{\lambda_\beta^2} + \frac{1}{8}\frac{\rho_2^2}{\lambda_\beta^2} + \Psi_1(\frac{\rho_1}{\lambda_\beta},\frac{\rho_2}{\lambda_\beta}) + \frac{\rho_1}{\lambda_\beta}[-\frac{\xi_1}{\lambda_\beta}\Psi_2(\frac{\xi_1}{\lambda_\beta},\frac{\xi_2}{\lambda_\beta}) + \frac{\zeta_1}{\lambda_\beta}\Psi_2(\frac{\zeta_1}{\lambda_\beta},\frac{\zeta_2}{\lambda_\beta})]$$
$$+ \frac{\rho_2}{\lambda_\beta}[\frac{\xi_2}{\lambda_\beta}\Psi_3(\frac{\xi_1}{\lambda_\beta},\frac{\xi_2}{\lambda_\beta}) - \frac{\zeta_2}{\lambda_\beta}\Psi_3(\frac{\zeta_1}{\lambda_\beta},\frac{\zeta_2}{\lambda_\beta})]\}, \tag{B8b}$$

where

$$\Psi_1(a,b) = \frac{a^2 - b^2}{r^2}[\frac{1}{2} + \frac{e^{-r}(r^2+3r+3)-3}{r^2}] - Ei(r) + \ln(r) + e^{-r} - 1 + \gamma, \tag{B9a}$$

$$\Psi_2(a,b) = \frac{1}{r^6}(a^4 + 6a^2 + 4a^2b^2 + 3b^4 - 18b^2) + e^{-r}\left[-2\frac{a^6}{r^7} - a^4(\frac{6}{r^7} + \frac{4}{r^6}) - 6\frac{a^2}{r^6} - 4\frac{a^4b^2}{r^7}\right.$$
$$\left. + 2a^2b^2(\frac{6}{r^7} + \frac{1}{r^6}) - 2\frac{a^2b^4}{r^7} + 6b^4(\frac{3}{r^7} + \frac{1}{r^6}) + 18\frac{b^2}{r^6}\right], \tag{B9b}$$

$$\Psi_3(a,b) = \frac{1}{r^6}(a^4 - 18a^2 - b^4 + 6b^2) + e^{-r}\left[2\frac{a^6}{r^7} + 2a^4(\frac{9}{r^7} + \frac{4}{r^6}) + 18\frac{a^2}{r^6} + 4\frac{a^4b^2}{r^7}\right.$$

$$+2\frac{a^2b^4}{r^7}+6a^2b^2\left(\frac{2}{r^7}+\frac{1}{r^6}\right)-2b^4\left(\frac{3}{r^7}+\frac{1}{r^6}\right)-6\frac{b^2}{r^6}\Big], \tag{B9c}$$

$r^2 = a^2+b^2$, Ei is the exponential integral, and γ is the Euler constant.

Appendix C: Expressions for the functions in Eq. (21)

$$\Xi_1(a,b)=-2\frac{9}{r^4}+\frac{1}{r^2}+e^{-r}\Big[a^2\left(\frac{2}{r^4}+\frac{2}{r^3}+\frac{1}{r^2}\right)-\frac{1}{r^2}-\frac{1}{r}\Big], \tag{C1}$$

$$\Xi_2(a,b)=-\frac{1}{2}\frac{1}{r^8}\Omega_1+\frac{e^{-r}}{r^9}\Omega_2+\frac{e^{-r}}{r^8}\Omega_3, \tag{C2}$$

where $r = (a^2+b^2)^{1/2}$,

$$\Omega_1(a,b)=a^6+3a^2b^2(-36+b^2)-3b^4(-6+b^2)+a^4(18+7b^2), \tag{C3}$$

$$\Omega_2(a,b)=2a^8+9b^6+a^6(9-2b^2)-5a^4b^2(9+2b^2)-3a^2b^4(15+2b^2), \tag{C4}$$

$$\Omega_3(a,b)=a^8+3b^4(3+b^2)+a^6(5+2b^2)-3a^2b^2(18+7b^2)+b^4(9-19b^2+b^4), \tag{C5}$$

Appendix D: Expressions for the functions in Eq. (22)

$$\Delta_1(a,b)=3a^8+4a^6(-1+3b^2)+b^4(72-4b^2+3b^4)+4a^2b^4(-108+5b^2+3b^4)+2a^4(36+10b^2+9b^4), \tag{D1}$$

$$\Delta_2(a,b)=-8a^8+4a^6\left[-18-8r+(8+2r)3b^2\right]+b^4\left[-72r-4(8+8r)b^2-8b^4\right]$$

$$+4a^2b^2\left[108r+5(18+8r)b^2+(8+2r)b^4\right]+2a^4\left[-36r+10(18+8r)b^2+(40+8r)b^4\right], \tag{D2}$$

$$\Delta_3(a,b)=a^8+4a^6b^2+b^4(144-16b^2+b^4)+4a^2b^4(-216+8b^2+b^4)+6a^4(24+8b^2+b^4), \tag{D3}$$

$$\Delta_4(a,b)=-8(3+r)a^8+4a^6\left[-18(2+r)+(12-2r)b^2\right]+b^4\left[-144r-8(18+7r)b^2-8b^4\right]$$

$$+4a^2b^2[216r+2(90+41r)b^2+(20+2r)b^4]+2a^4[-72r+12(30+13r)b^2+(80+4r)b^4], \qquad \text{(D4)}$$

where $r = (a^2+b^2)^{1/2}$.

Data availability. No data was used for the research described in the article.

Author contributions. C-MC: Conceptualization, Methodology, Formal analysis, Writing - original draft preparation, Writing - review & editing.

C-FN: Conceptualization, Methodology, Formal analysis, Writing - original draft preparation, Writing - review & editing, Supervision, Funding acquisition.

C-PL: Conceptualization, Methodology, Formal analysis, Writing - original draft preparation, Writing - review & editing.

I-HL: Conceptualization, Methodology, Formal analysis, Writing - original draft preparation, Writing - review & editing.

Competing interests. The authors declare that they have no conflict of interest.

Acknowledgements. Research leading to this paper has been partially supported by the grant from the Taiwan Ministry of Science and Technology under the grants MOST 108-2638-E-008-001-MY2, MOST 110-2123-M-008-001-, MOST 110-2621-M-008-003-, and MOST 110-2811-M-008-533. We are grateful to the Editor Prof. Monica Riva and anonymous referees for constructive comments that improved the quality of the work.

References

Bailey, R. T. and Baù, D.: Estimating geostatistical parameters and spatially-variable hydraulic conductivity within a catchment system using an ensemble smoother, Hydrol. Earth Syst. Sci., 16(2), 287-304, 2012.

Bear, J.: Hydraulics of groundwater, McGraw-Hill, New York, 1979.

Bear, J. and Cheng, A.H.-D.: Modeling groundwater flow and contaminant transport, Springer, Dordrecht, 2010.

Butera I. and Tanda, M.: Solute transport analysis through heterogeneous media in nonuniform in the average flow by a stochastic approach, Transp. Porous Media, 36(3), 255-291, 1999.

Butera, I., Cotto, I., and Ostorero, V.: A geostatistical approach to the estimation of a solute trajectory through porous formations, J. Hydrol., 375(3-4), 345-355, 2009.

Chang, C-M, Ni, C-F, Li, W-C, Lin, C-P, and Lee, I-H: Stochastic analysis of the variability of groundwater flow fields in heterogeneous confined aquifers of variable thickness, Stoch. Environ. Res. Risk Assess., https://doi.org/10.1007/s00477-021-02125-7, 2021.

Chile`s, J. P. and Delfiner, P.: Geostatistics: modeling spatial uncertainty, 1^{st} ed., Wiley-Interscience, New York, 1999.

Ciriello, V. and Barros, F. P. J.: Characterizing the influence of multiple uncertainties on predictions of contaminant discharge in groundwater within a Lagrangian stochastic formulation, Water Resour. Res., 56(10), doi:10.1029/2020wr027867, 2020.

Cuello, J. E. and Guarracino, L.: Tide-induced head fluctuations in coastal aquifers of variable thickness, Hydrol. Process., 34, 4139-4146, 2020.

Cvetkovic, V., Fiori, A., and Dagan, G.: Tracer travel and residence time distributions in highly heterogeneous aquifers: Coupled effect of flow variability and mass transfer, J. Hydrol., 543(Part A), 101-108, 2016.

Dagan, G.: Stochastic modeling of groundwater flow by unconditional and conditional probabilities: 2. The solute transport, Water Resour. Res., 18(4), 835-848, 1982.

Dagan, G.: Solute transport in heterogeneous porous formation, J. Fluid Mech., 145, 151-177, 1984.

Dagan, G.: Flow and transport in porous formations, Springer, New York, 1989.

de Marsily, G.: Quantitative hydrogeology: Groundwater hydrology for engineers, Academic Press, Orlando, FL, 1986.

DeSimone, L. A., Pope, J. P., and Ransom, K. M.: Machine-learning models to map pH and redox conditions in groundwater in a layered aquifer system, Northern Atlantic Coastal Plain, eastern USA, J. Hydrol. Reg. Stud., 30, 100697, 2020.

Fischer, H. B., List, E. J., Koh, R., Imberger, J., and Brooks, N.: Mixing in inland and coastal waters, Academic, San Diego, 1979.

Gelhar, L. W.: Stochastic Subsurface Hydrology, Prentice Hall, Englewood Cliffs, New Jersey, 1993.

Guadagnini, A. and Neuman, S. P.: Nonlocal and localized analyses of conditional mean steady state flow in bounded, randomly nonuniform domains: 2. Computational examples, Water Resour. Res., 35, 3019-3039, 1999.

Gutjahr, A. L. and Gelhar, L. W.: Stochastic models of subsurface flow: infinite versus finite domains and stationarity, Water Resour. Res., 17(2), 337-350, 1981.

Hantush, M. S.: Flow of ground water in sands of nonuniform thickness, part 3. Flow to wells, J. Geophys. Res., 67(4), 1527-1534, 1962.

Holly, F. M. JR.: Two-dimensional mass dispersion in rivers, Hydrology Papers, No. 78., Colorado State University, Fort Collins, 1975.

Jing, M., Heße, F., Kumar, R., Kolditz, O., Kalbacher, T., and Attinger, S.: Influence of input and parameter uncertainty on the prediction of catchment-scale groundwater travel time distributions, Hydrol. Earth Syst. Sci., 23(1), 171-190, 2019.

Lumley J. L. and Panofsky, H. A.: The structure of atmospheric turbulence, John Wiley, New York, 1964.

Masterson, J. P, Pope, J. P., Monti, J., Nardi, M. R., Finkelstein, J. S., and McCoy, K. J.: Hydrogeology and hydrologic conditions of the Northern Atlantic Coastal Plain aquifer system from Long Island, New York, to North Carolina, US Geol. Surv. Sci. Invest Rep., 2013-5133, 2013.

Matheron, G.: The intrinsic random functions and their applications, Adv. Appl. Probab., 5(3), 439-468, 1973.

Risken, H.: The Fokker-Planck equation, Springer, New York, 1989.

Rubin, Y. and Bellin, A.: The effects of recharge on flow nonuniformity and macrodispersion, Water Resour. Res., 30(4), 939-948, 1994.

Rubin, Y.: Applied Stochastic Hydrogeology, Oxford University Press, New York, 2003.

Van Kampen, N. G.: Stochastic processes in physics and chemistry, North-Holland, Amsterdam, 1992.

Zamrsky, D., Oude Essink, G. H., and Bierkens, M. F.: Estimating the thickness of unconsolidated coastal aquifers along the global coastline, Earth Syst. Sci. Data, 10(3), 1591-1603, 2018.

Zhang, D. and Winter, C. L.: Moment equation approach to single phase fluid flow in heterogeneous reservoirs, Soc. Petrol Eng. J., 4, 118-127, 1999.